

PERFORMANCE-BASED ANALYSIS OF PLANAR STEEL FRAME IN FIRE

The Effect of Different Types of Thermal Insulation

Anita Treven^a, Tomaž Hozjan^a, Miran Saje^a

^a University of Ljubljana, Faculty of Civil and Geodetic Engineering, Ljubljana, Slovenia

Abstract

The paper presents a performance-based analysis of a planar steel frame exposed to natural fire conditions, if protected with different types of insulation. Bare steel elements, and elements protected with intumescent coating or insulation boards are considered. Two fire scenarios and two material models for steel, with and without the consideration of viscous creep, are applied in order to observe the effect of viscous creep. The analysis consists of three steps: (i) the determination of fire curves, (ii) the thermal analysis, and (iii) the mechanical analysis. The expansion of intumescent coating as well as heat flux within the void space between the steel surface and the insulation boards are also considered. It is shown that the choice of the thermal insulation has a significant effect on the mechanical response of the frame.

Keywords: planar steel frame, real fire, intumescent coating, insulation boards, viscous creep

1 INTRODUCTION

The paper presents a performance-based analysis of a planar steel frame exposed to natural fire conditions. The main objective of the study is to determine whether different types of fire protection have substantially different effect on mechanical behaviour of the frame. Bare elements, and elements protected with intumescent coating or protected with insulation boards are considered and their effects compared. Temperature dependent thermal properties of fire protection materials, especially those of intumescent coatings, are hardly known, as they are not only difficult to obtain experimentally, but they are also very manufacturer-specific. For a 1-D heat flux and well-defined external conditions, a theoretical model for predicting an expansion rate of intumescent coating was developed in (Zhang et al, 2012). The thermal conductivity of intumescent coating was determined for a 1-D heat flux (Berg and Opstad, 2010) and for a 2-D heat flux for some standard steel profiles (Kolšek and Češarek, 2015) by fitting it to the experimental results, such that the thickness and the heat capacity remained constant. Knowledge of these properties is necessary for a proper performance-based analysis.

The analysis is divided in three separate steps. During the first step, two natural fire curves are obtained by the zone model Ozone (Cadorin et al, 2009). Both fire curves reach the same maximum temperature, but differ in duration. It is well known that, for temperatures above 400°C, steel elements experience significant time-dependent deformations, which is due to viscous creep. The use of thermal insulation delays both heating and cooling of steel and can therefore amplify the differences in the mechanical response of a structure between different fire scenarios.

The second step consists of the thermal analysis, where the distribution of temperatures over cross-sections of the frame as a function of time is evaluated. The insulation is modelled in the thermal analysis as an integral part of the cross-section with appropriately assigned material properties. Fourier's law of heat conduction is employed for the calculation of heat flux in the steel profile and in the insulation material. The insulation boards form an encasement around the steel profile, which results in a possible void space between the boards and the profile. Within the void, the heat flux due to the radiation and convection is taken into account, using simplified formulae (Velikanje, 1993).

The thermal analysis is followed by the mechanical analysis, performed with the strain-based finite elements. Here, the insulation is considered as a non-bearing part of the profile. Two material models of steel at elevated temperatures are employed, the European standard EC3 model as well

asthe bilinear elasto-plastic model combined with the Williams-Leirviscous creep model (Williams-Leir, 1983).

2 GENERAL INFORMATION ABOUT THE ANALYSED FRAME

The analysed steel planar frame consists of two columns with standard profile HEA 200, which are 4 m high, and a beam, whose length is 8 m. The beam's profile is that of a British universal beam 305x165x40. All joints and restraints are fully rigid. The permanent load on the beam with characteristic value 14.42 kN/m includes the beam's and the concrete slab's self-weight. The weight of a fire protection material is assumed to be negligible. The characteristic value of the imposed load due to snow is 3.03 kN/m, in accordance with EC1-3 for a building with flat roof and altitude 300 m above the sea level. The frame is subjected to a compartment fire, which affects all sides of the columns and three sides of the beam, since the upper side of a beam is protected by the concrete slab.

3 STEP 1: DETERMINATION OF FIRE CURVES

The two natural fire curves are determined by the zone model OZONE, which is in accordance with the EN 1991-1-2. In order to assess fire scenarios with different duration of temperatures above 400°C, yet similar in other aspects, only ventilation and fire protection measures are altered. Therefore, both fires have the same maximum fire area of 48 m², surrounded by 4 m high concrete walls with length of 8 m and 6 m. The selected fire growth rate and danger of fire activation are medium, with fire load $q_{f,k}=500$ MJ/m². Rate of the heat release density, RHRf=250 kW/m², corresponds to an office use. The full list of differences between the selected fire curves is presented in Table 1.

Table 1 The differences between the selected fire curves

	Fire curve F1	Fire curve F2
Assumed ventilation and fire protection measures		
Dimensions of a window (height x length)	3 m x 3 m	3 m x 3.5 m
Off-Site Fire Brigade	✓	x
Firefighting Devices	✓	x
Smoke Exhaust System	✓	x
Safe Access Routes	x	✓
Staircases under Overpressure in Fire Alarm	x	✓
Main characteristics of the fire curves		
Maximum temperature T_{max}	715 °C	715 °C
$t(T_{max})$	38 min	58 min
Approximate duration of $T > 400$ °C	42 min	71 min

The observed time is 200 min. The graph of the variation of temperature with time is shown in Figure 1. As the modelled fire compartment is selected to be only one fire zone, the same fire curve applies to the entire steel frame.

4 STEP 2: THERMAL ANALYSIS

The temperature is assumed to be constant over the entire compartment; consequently each construction element assumes the same temperature distribution in any cross-section over the length. For each of the fire curves, the thermal analysis is conducted for each possible combination of the construction element and the insulation: uninsulated column (c-UN), column with intumescent coating (c-IC) and with insulation boards (c-IB), uninsulated beam (b-UN), beam with intumescent coating (b-IC) and with insulation boards (b-IB). A 2-D distribution of temperatures across the selected cross-sections is evaluated with the computer program Heatko, based on the finite element

method. Fourier's law of heat conduction is employed for the calculation of heat flux through the finite elements. The heat flux due to the fire radiation is taken into account both on the external surfaces of the profile, as well as on the internal surfaces of the voids. The heat flux due to the convection is accounted for on all surfaces using the convection coefficient $h_c=25$ for external surfaces of the cross section, if exposed to the fire, and $h_c=9$ for the internal and non-exposed external surfaces. Thermal properties of steel are taken in accordance with EC3 and are the same for unprotected steel profiles as well as for those protected with insulation boards or intumescent coating. Since the insulation is modelled as an integral part of the cross-section with appropriately assigned material properties, voids can be formed between the insulation boards and the profile. Further details on modelling each particular insulation material are given in the following subsections. Furthermore, an average of the temperatures evaluated in the nodes of the finite elements, belonging to the steel profile, is calculated and made ready for the use in the mechanical analysis.

4.1 Modelling of Intumescent Coating

There are several further issues that need to be addressed for a proper modelling of an intumescent coating. Firstly, the temperature at which the expansion takes place and the final thickness of the coating after an expansion to d_{end} is completed have to be determined. The latter highly depends, among other conditions, on a dry film thickness (DFT) of intumescent coating. In Eq. (1) we propose a simple formula for estimating the final thickness of intumescent coating:

$$d_{end} [\text{mm}] = \begin{cases} 34\sqrt{DFT [\text{mm}]}, & DFT < 1 \text{ mm} \\ 34 DFT [\text{mm}], & DFT \geq 1 \text{ mm} \end{cases} \quad (1)$$

The graphical presentation of the formula in Figure 1 shows a good agreement with the experimental results (Zhang et al, 2012).

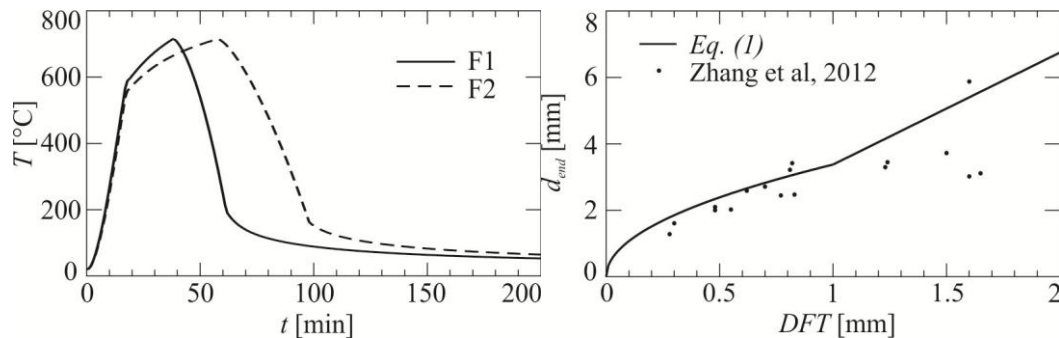


Fig. 1 Fire curves (left) and comparison of analytical prediction of d_{end} with experimental results (right)

During the expansion and after it is completed, the finite element mesh of the steel profile remains the same. By contrast, when the nodes on the external edge, belonging to the coating, reach the temperature of 275°C, they instantaneously move further away from the profile, so that one half of the required thickness of the coating $0.5d_{end}$ is realized. Only when they reach temperature 375 °C, the final thickness d_{end} is realized. The temperatures at which the expansion occurs, and the corresponding thermal conductivity of the expanded intumescent coating, are fitted to the experimental results by (Kolšek and Češarek, 2015) using the trial and error method, while the heat capacity and the density are kept constant, with values of 840 J/kgK and 1600kg/m³, respectively. The thermal conductivity, λ , is temperature-dependent and its values vary with the section factor, A_m/V . The values of the thermal conductivity at characteristic temperatures are given in Table 2. The linear interpolation is applied in-between.

Table 2 Temperature dependent thermal conductivity of intumescent coating

T [°C]	0	300	400	600	700	>900
λ beam [W/mK]	2.4	2.4	0.66	0.66	2	2.8

λ column [W/mK]	1.32	1.32	0.363	0.363	1.1	1.54
-------------------------	------	------	-------	-------	-----	------

After the cooling phase begins and the temperatures in the intumescent coating start falling, it is assumed that the thermal conductivity of the intumescent coating remains constant.

A close fit of our numerically obtained temperatures in the steel profile with experimental results by (Kolšek and Češarek, 2015), during the heating phase is shown in Figure 2. The column was exposed to ISO 834 fire curve at all four sides, and was tested for four DFT s. The results with $DFT=0.9$ mm were chosen in the further analyses. The beam, on the other hand, was exposed at only three sides to ISO 834 fire curve including the cooling phase, which started after 45 min, and had $DFT=1$ mm.

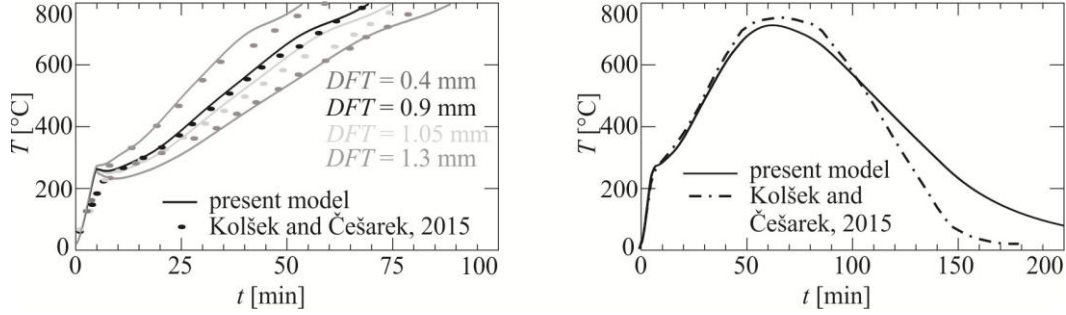


Fig. 2 The comparison of average temperatures in steel profile obtained by the present numerical model and the experimentally obtained temperatures (Kolšek and Češarek, 2015)

As there are many intumescent coatings available in the market that vary significantly regarding the chemical composition, we would like to emphasize the fact that the results are valid only for the coatings presented in (Kolšek and Češarek, 2015).

4.2 Modelling Insulation Boards

According to the manufacturers, the insulation boards have temperature-independent density, heat capacity and thermal conductivity. Experimental researches have shown, that this is not entirely correct, though (Rahmanian and Wang, 2009). Nevertheless, density, heat capacity, and thermal conductivity for the present analysis are chosen to be 700 kg/m^3 , 880 J/kgK and 0.189 W/mK , respectively, which corresponds to PROMATECT 200 insulation boards. The heat flux within a possible voidspace between the steel profile and the insulation boards, is the sum of the heat flux due to the radiation, q_r , and the heat flux due to the convection, q_c , and appears to be a very complex process. As a simplification it is presumed, that the temperature is equal within the whole void space and is determined by solving Eq. (2) iteratively:

$$\rho_a c_a V_a \frac{T_a^i - T_a^{i-1}}{\Delta t} = \int_0^L \left(h_c + \varepsilon \sigma \left(T_e^{i-1^2} + T_a^{i-1^2} \right) \left(T_e^{i-1} + T_a^{i-1} \right) \right) \left(T_e^{i-1} - \frac{T_a^{i-1} + T_a^i}{2} \right) ds \quad (2)$$

Here ρ_a , c_a , and V_a are density, heat capacity and volume of the air within the void space, respectively. L is length of the edge of the void space, h_c is the coefficient of convection, Δt is the time increment, ε is the emissivity of the black body, and σ is the Stefan-Boltzmann constant. T_a is the temperature of air within the void space, and T_e is the temperature along the edge. The thickness of the insulation board is selected such that the coefficient of protection of the steel profile $k_p = (\lambda_p/d_p)(A_p/V)$ (Franssen and Zaharia, 2006) is the same for protection with the insulation boards as well as for the protection with intumescent coating. Here λ_p and d_p are thermal conductivity and thickness of the insulation material, respectively, and A_p/V is the section factor for protected sections. Hence, the column is protected at all four sides by 6.45 mm thick insulation boards. The equivalent thickness of the insulation boards on the beam is 3.65 mm. Average temperatures within the beam steel profile for the two fire curves and all various insulations are shown in Figure 3.

5 STEP 3: MECHANICAL ANALYSIS

The mechanical analysis is performed with program POZAR for analysing planar frames at time-dependent temperatures, which uses strain-based finite elements. The program was developed and validated by (Hozjan et al, 2007). The Lobatto numerical integration of 5th order is applied, and time increment of 30 s is selected. The geometry of the frame is as described in Section 1. The mechanical load is evenly distributed along the beam, with the total value 20 kN/m, which represents 83.3% of the value obtained for the load combination of actions for a persistent design situation according to EC0. The mechanical properties of steel at elevated temperatures are firstly taken in accordance with EN 1993-1-2, where viscous creep deformations are not explicitly considered and hence the actual duration of high temperatures does not affect the mechanical response of the structure.

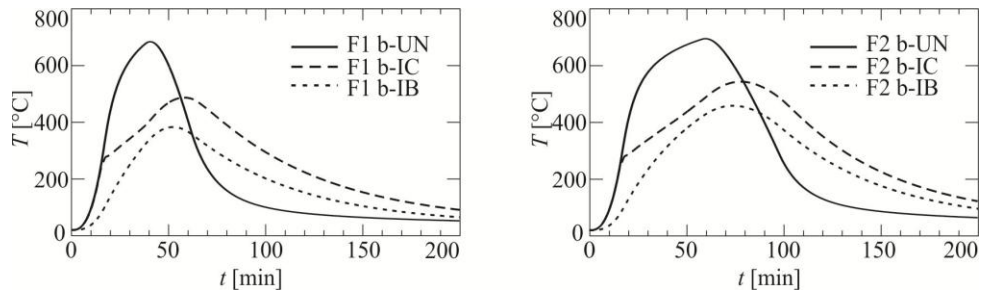


Fig. 3 Average temperatures within the beam steel profile for different fire curves and types of insulation

The second material model considered here proposes, in accordance with the French regulations, the bilinear stress-strain diagram. Additionally, the Williams-Leir viscous creep model (Williams-Leir, 1983) is employed. The selected set of coefficients for this kind of analysis corresponds to steel type A135, whose time-dependent viscous creep deformations are about average, regarding the existing sets of coefficients (Hozjan et al, 2007).

6 RESULTS AND DISCUSSION

For two fire curves (fast F1 and slow F2), three types of fire protection (none, intumescent coating and insulation boards), and two material models (EC3 and bilinear with the viscous creep), the midpoint deflection of the beam is compared. The graphs in Figure 4 show the variation of the deflection with time (left) and with temperature (right). For the unprotected frame, there exists only a small difference in the mechanical response of the construction, for various fire curves and material models. Here, the frame fails at around 25 min after the fire starts. Within this time interval, the fire curves and, consequently, temperatures in steel profiles are almost identical. Also, as the rise of the temperatures in the steel profiles is very quick, see Figure 3, the viscous creep deformations do not have time to develop. Substantial displacements in the protected beam develop only much later. When the beam is protected with the intumescent coating, the stresses are beneficially redistributed and the frame does not fail only in the combination of the fire curve F1 and the EC3 material model. When the beam is protected with the insulation boards, the frame fails only in the case of slow fire F2 and the bilinear material model enhanced by the viscous creep deformations. It can be noted that the temperatures, at which high displacements occur, are lower for the bilinear material model including viscous creep deformations than for the EC3 material model. For both material models we can observe that the temperatures are much lower for the protection with insulation boards, than for the protection with intumescent coating, although they are reached at roughly the same time for both types of the protection.

7 CONCLUSIONS

According to the presented results, different types of fire protection have different effects on the mechanical response of the frame. It appears that the protection of the frame with the insulation boards allows a better stress redistribution and may prevent failure of the frame in some cases. By

contrast, the protection with the equivalent intumescent coating is not so successful. However, there is plenty of room for further investigations, particularly in a more accurate modelling of phenomena concerned with the expansion of the intumescent coating and heat transfer within the voids between the steel profile and the insulation boards.

ACKNOWLEDGMENTS

This work was supported by the Slovenian Research Agency through grant 1000-14-0510 in accordance with decision No. 1240-1/2013-49. The support is gratefully acknowledged.

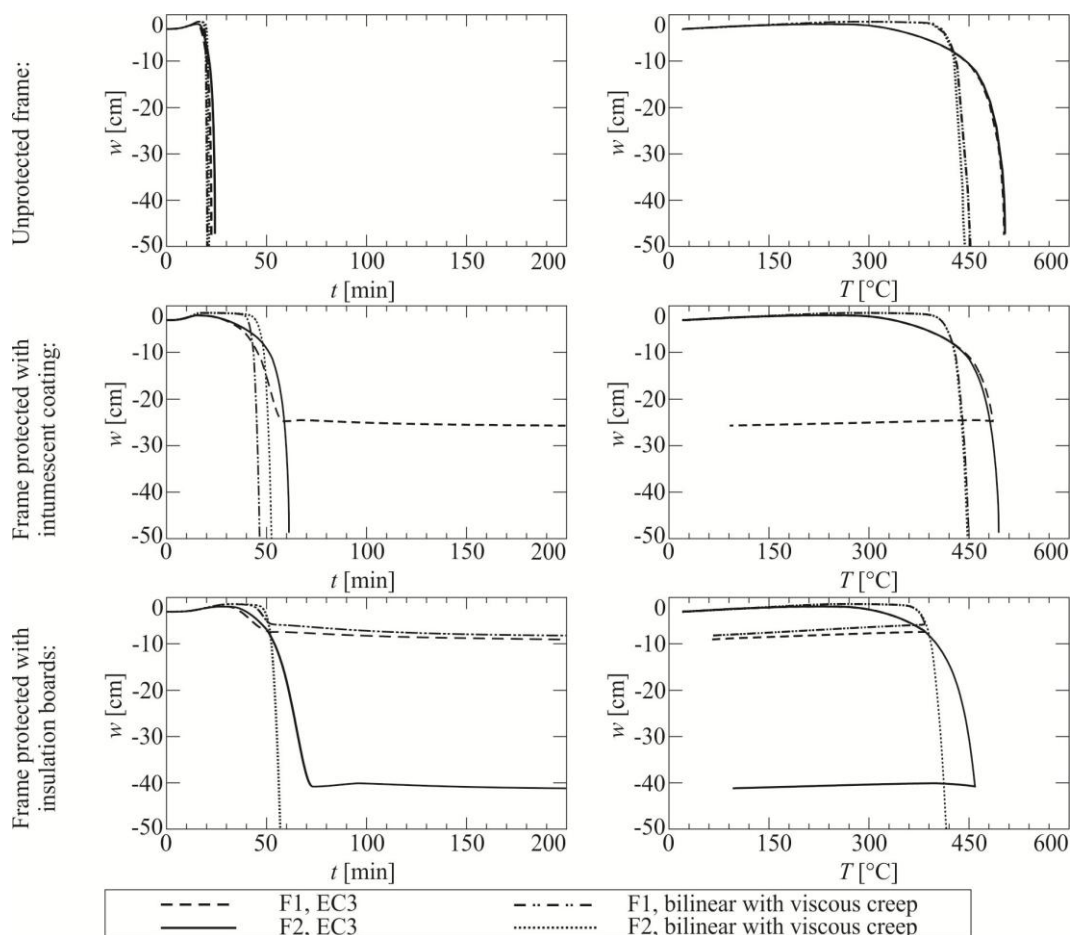


Fig. 4 The mid-point deflection of the beam

REFERENCES

- Berge G., Opstad K. 2010. Thermal Properties of Intumescent Passive Fire Protection Materials, in *4th International Conference on Safety & Environment in Process Industry*, 14-17 March 2010, Florence, Italy, p. 217-242.
- Cadorin J. F., Franssen J-M., Pintea D. I. 2009. *Ozone V2.2*. Liège, Belgium: University of Liège.
- EN 1991-1-2, Eurocode 1, Actions on Structures – Part 1-2: General actions – Actions of structures exposed to fire. Brussels: European Committee for Standardisation, 2002.
- EN 1993-1-2, Eurocode 3, Design of steel structures – Part 1-2: General rules - structural fire design. Brussels: European Committee for Standardisation, 2005.
- Franssen J-M., Zaharia R. 2006. *Design of Steel Structures subjected to Fire, Background and Design Guide to Eurocode 3*, Liège, Belgium: University of Liège.
- Hozjan T., Turk G., Srpčič S. 2007. *Fire analysis of steel frames with the use of artificial neural networks*. *Journal of Constructional Steel Research*, 63, p. 1396-1403.
- Kolšek J., Češarek P. 2015. *Performance-based fire modelling of intumescent painted steel structures and comparison to EC3*. *Journal of Constructional Steel Research*, 104, p. 91-103.
- Rahmanian, I., Wang, Y. 2009. *Thermal Conductivity of Gypsum at High Temperatures, A Combined Experimental and Numerical Approach*. *Acta Polytechnica*, 49, p. 16-20.

- Velikanje, B. 1993. *Vpliv temperature na mostove*, Master Thesis, University of Ljubljana (in Slovenian).
- Williams-Leir, G. 1983. *Creep of Structural steel in fire: Analytical expressions*. *Fire and Materials*, 7, 2: p. 73-78.
- Zhang Y., Wang Y.C., Bailey C.G., Taylor A.P. 2012. *Global modelling of fire protection performance of intumescent coating under different cone calorimeter heating conditions*. *Fire Safety Journal*, 20, p. 51-62.